Supporting Information: Revisiting the active sites at the MoS_2/H_2O interface via grand-canonical DFT: The role of water dissociation

Nawras Abidi,[†] Audrey Bonduelle-Skrzypczak,[‡] and Stephan N. Steinmann[*,†]

†*Univ Lyon, Ens de Lyon, CNRS UMR 5182, Université Claude Bernard Lyon 1, Laboratoire de Chimie, F69342, Lyon, France*

‡*IFP Energies nouvelles, Rond-point de l'échangeur de Solaize, 69360 Solaize, France*

E-mail: stephan.steinmann@ens-lyon.fr

Phone: (+33)4 72 72 81 55

Contents

1 Stability of the different MoS_2 polytypes

As mentioned in the literature[S1], among the 3 polytypes, only 2H and 3R are stable. The physical and chemical properties of polytype 3R are almost identical to those of polytype 2H. These two stable polytypes of MoS_2 are found in nature and are mainly obtained by mining. The majority (80%) of natural molybdenite has a 2H stack, and only 3% of the ore is purely of the 3R type.[S2] The rest exists as a mixture. On the other hand, 1T is metastable and is found in synthetic MoS_2.[S3] The DFT computations suggest the appearance of two different types of superstructures following the distortion of octahedra in 1T phase. These new structures are 1T' and 1T" with different elementary cells. In these distorted structures, Mo-Mo associations take place. The dimerization of Mo atoms gives the structure 1T' and the trimerization of Mo atoms gives 1T" and the new systems obtained are semi-conducting.[S4] This is not the case for 1T which is metallic.[S5] Therefore, the distorted phases loose the interest of high electronic mobility of the 1T-phase in the context of electrocatalysis. In agreement with the general observations for Peierls distortions, they decrease the total energy of the structures compared to the primitive

structure 1T. 1T′ turns out to be the most stable phase.[S6]

1.1 Defect formation

Vacancies V_S and V_{S2} have the lowest formation energy respectively, and the 2H structure retains its trigonal prismatic coordination (see Table S1). This confirms the stability of this polytype unlike the different polymorphs of 1T, which become more and more unstable in the presence of the defects, i.e., undergoes significant distortions, leading to further gap-openings and formation energies that are heavily influenced by the surface reconstruction energy. Even for 1T′, which has the most stable bulk, there is a strong deformation of the surface upon defect introduction.

Table S1: Formation energy of the different type of defects

Type of defect	Formation energy (eV)
V_S	2.29
V_{S2}	4.78
Mo_S	7.20
Mo_{S2}	8.26
Mo_{S2*}	9.19

2 Additional Figures and Tables

2.1 Hydrogen adsorption on the perfect basal plane

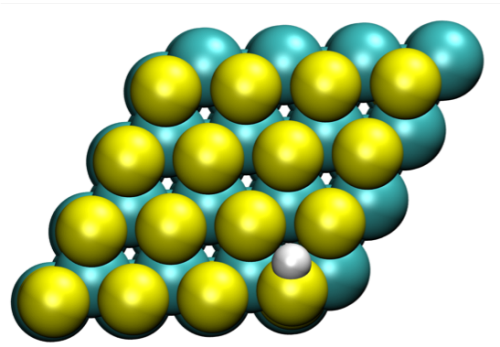

Figure S1: Adsorption of hydrogen on the perfect basal plane with an adsorption free energy at 0 V equal to **1.67 eV**.

2.2 Hydrogen adsorption on the defects in vacuum

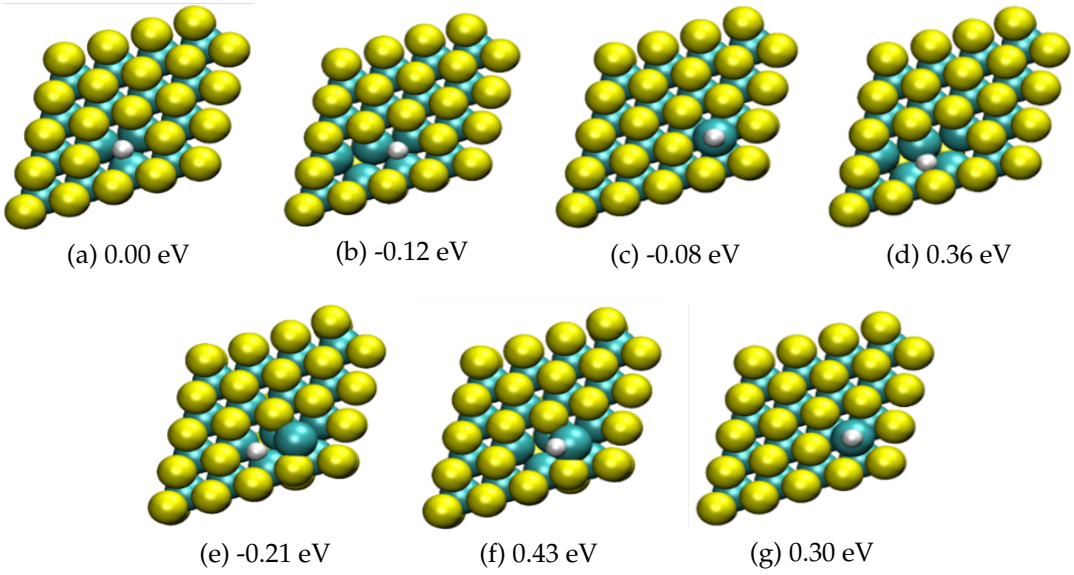

(a) 0.00 eV (b) -0.12 eV (c) -0.08 eV (d) 0.36 eV

(e) -0.21 eV (f) 0.43 eV (g) 0.30 eV

Figure S2: Adsorption of H on: (a) V_S, (b) V_{S2}, (c) Mo_S, (d) V'_{S2}, (e) Mo_{S2}, (f) Mo'_{S2}, (g) Mo_{S2*}.

2.3 Hydrogen adsorption on the defects in aqueous medium

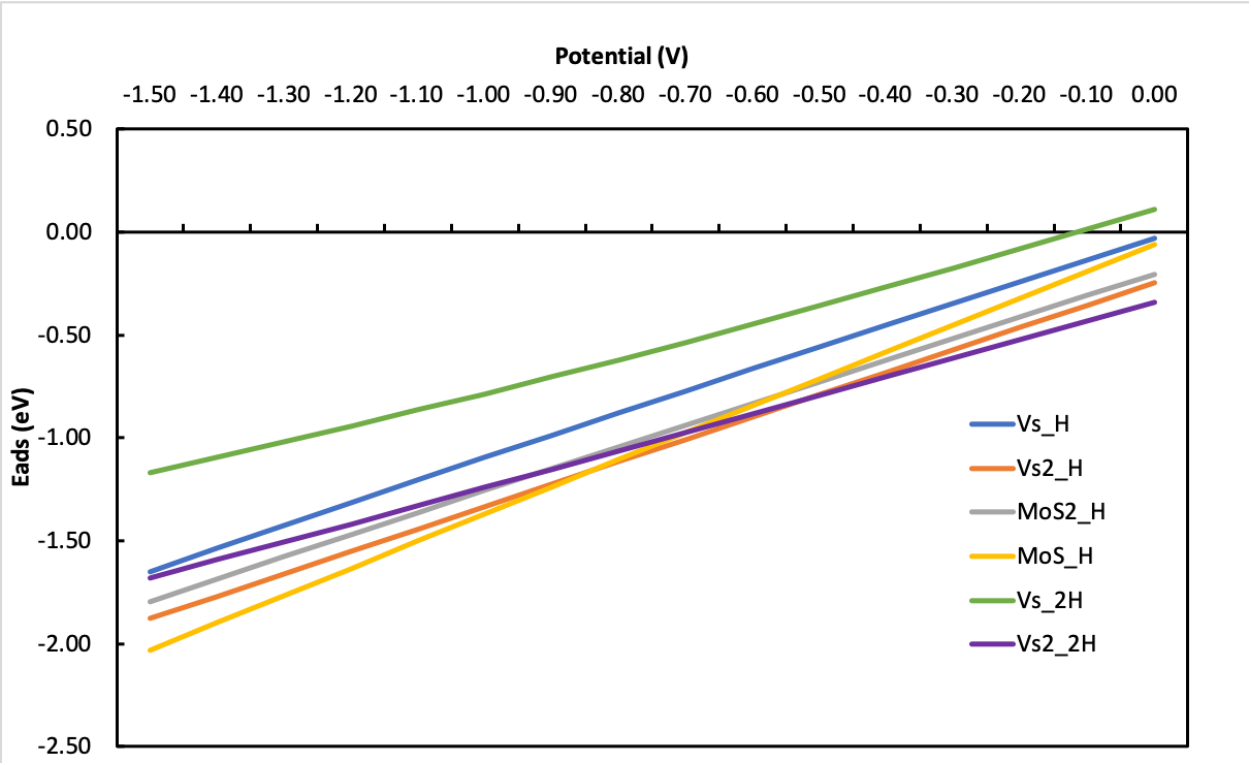

Figure S3: Variation of the adsorption energy of the hydrogen on the different defects as a function of the electrochemical potential

2.4 Water molecule adsorption on the defects

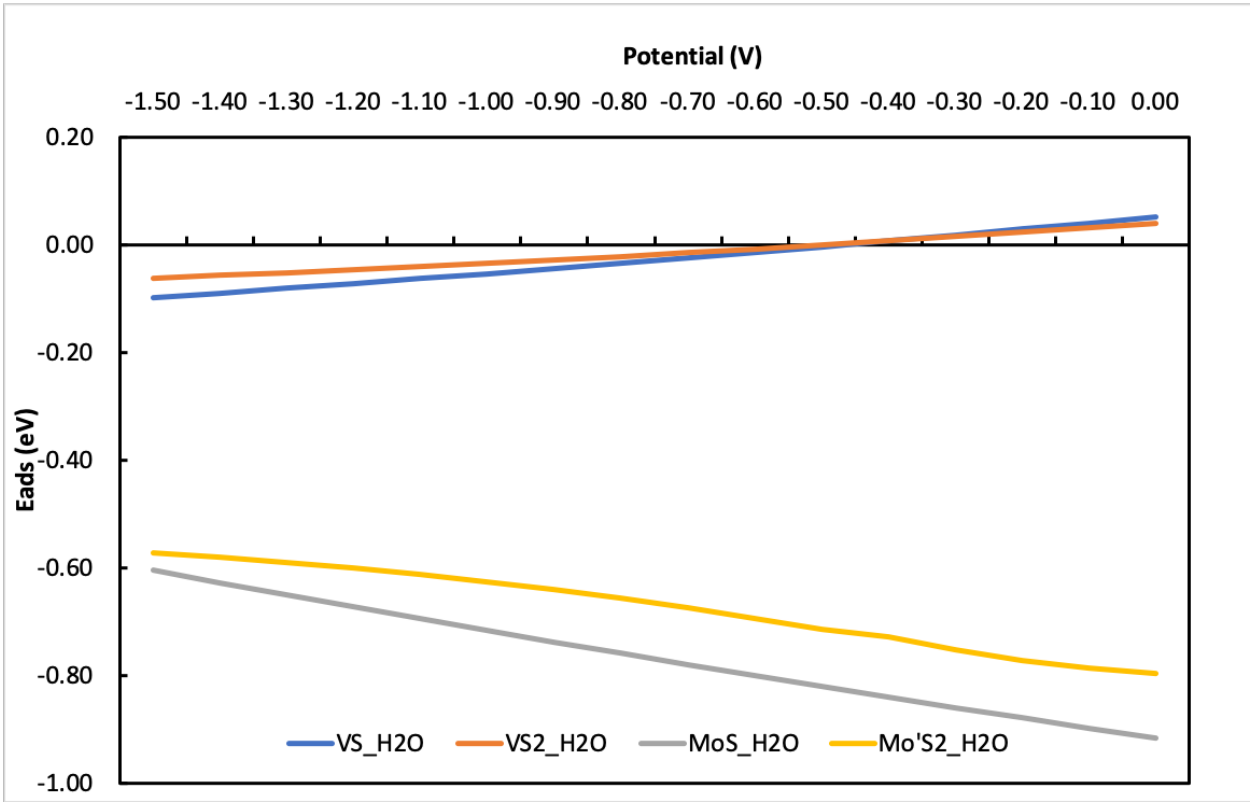

Figure S4: Variation of the adsorption energy of the water molecule on the different defects as a function of the electrochemical potential

2.5 OH adsorption on the defects

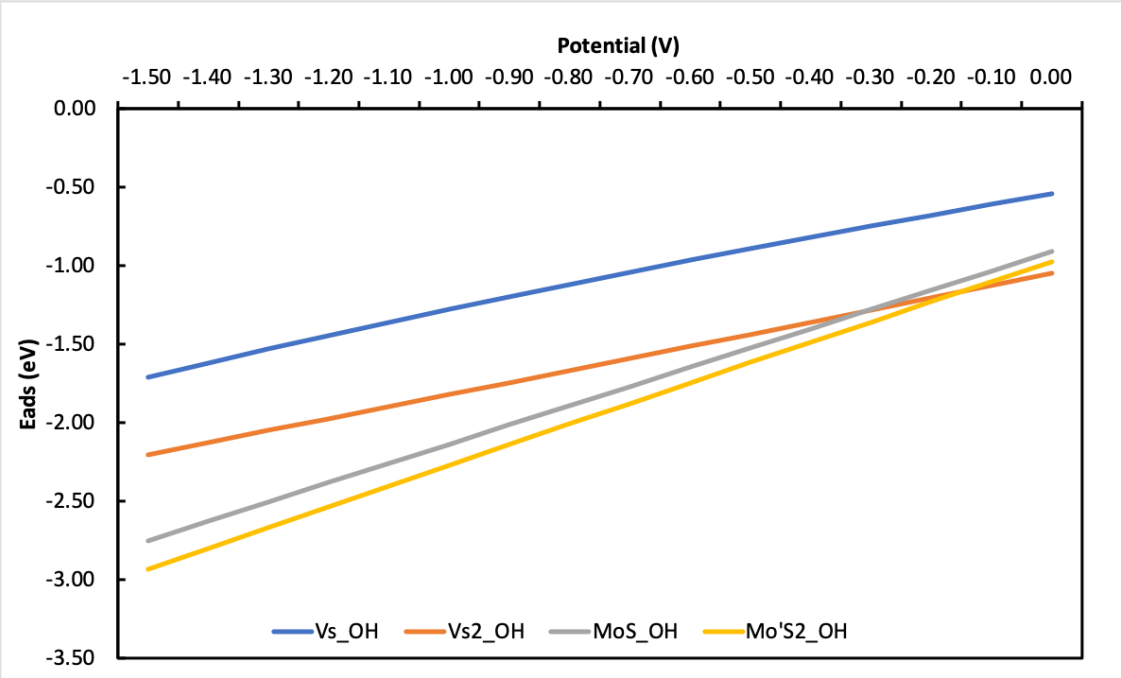

Figure S5: Variation of the adsorption energy of the OH on the different defects as a function of the electrochemical potential: For all the sites: V_S, V_{S2}, Mo_S, Mo'_{S2}, OH is strongly adsorbed (-0.55 eV, -1.05 eV, -0.91 eV and -0.97 eV respectively).

2.6 Hydrogen adsorption on Mo-edges and S-edges

We start with the adsorption of the hydrogen on different sites of the 2H-MoS_2: Top S, Top Mo and Bridge. Computations without electrochemical potential done at first have indicated that the Hollow site is catalytically inert. As expected for a reduction reaction, the free energies of hydrogen adsorption are observed to increase (see Figure S6) with increasing potential.

According to Fig. S6 all active sites can bind the first hydrogen adsorbate. Top S and Top Mo have approximately the same adsorption energy (-0.44 eV and -0.43 eV respectively) and the Bridge site is seen to yield the strongest hydrogen adsorption energy (-0.78 eV). The first two sites could be considered active, whereas the adsorption energy of the hydrogen on the Bridge site is not in the acceptable range anymore since it is too strong.

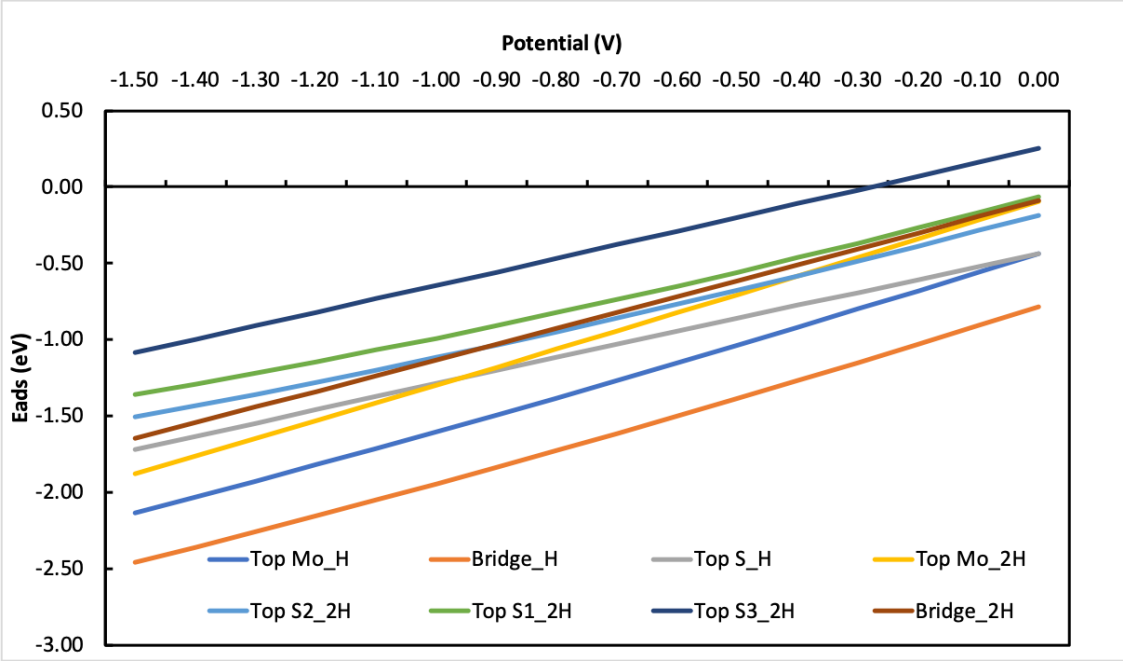

Figure S6: Variation of the adsorption energy of the hydrogen on the different edge sites as a function of the electrochemical potential

At first sight, we note that only certain sites on the 2H-MoS_2 edges are responsible for the electrocatalytic activity of the 2H-MoS_2. However, considering higher hydrogen coverages change the picture. Indeed, all the sites become promising from the catalytic point of view with adsorption energies very close to 0 eV, especially Top Mo, Bridge and Top S1 (-0.1 eV, -0.09 eV and -0.06 eV respectively). Top S2 and Top S3 are less likely to generate H_2 with adsorption energies a little further from 0 eV (-0.18 eV and 0.25 eV).

As a conclusion, our results are well in line with previous studies in which 2H-MoS_2 edges have been deemed as catalytically active.

2.7 Water molecule adsorption on Mo-edges and S-edges

2.7.1 Adsorption of the first water molecule on Mo-edges and S-edges

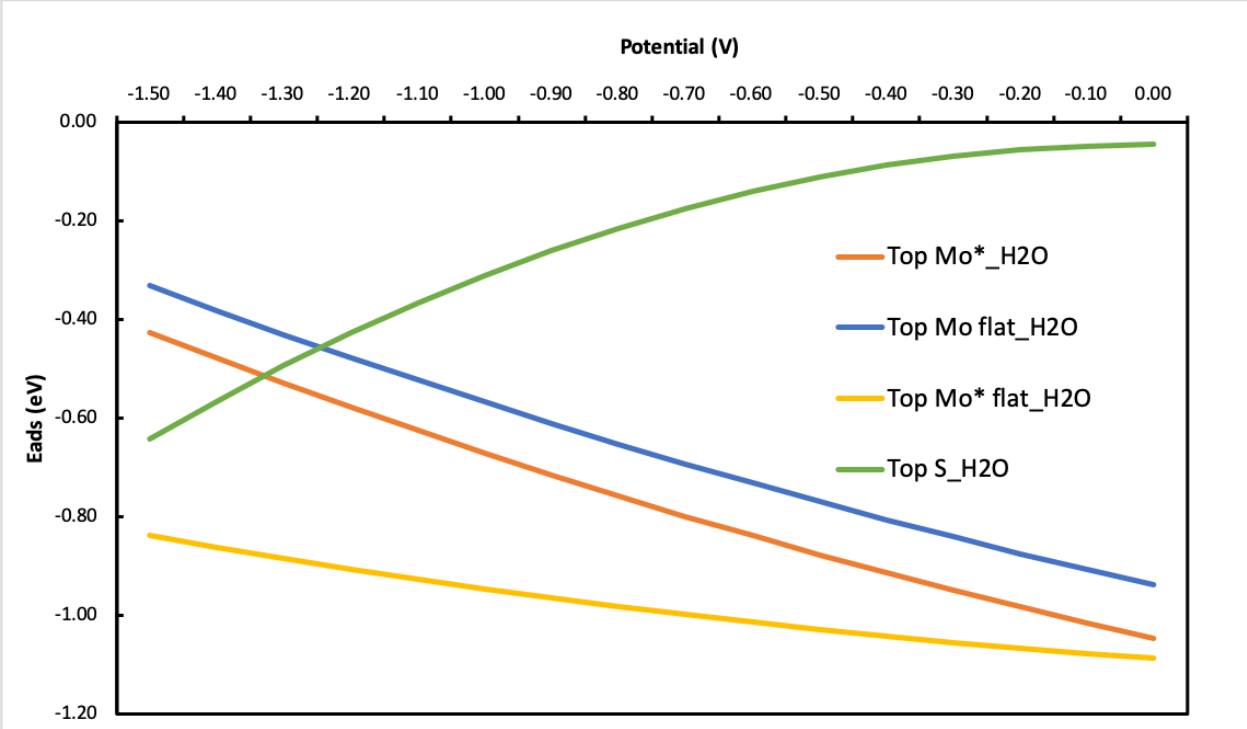

Figure S7: Variation of the adsorption energy of the water molecule on the different edge sites as a function of the electrochemical potential.

2.7.2 Adsorption of the second water molecule on Mo-edges and S-edges

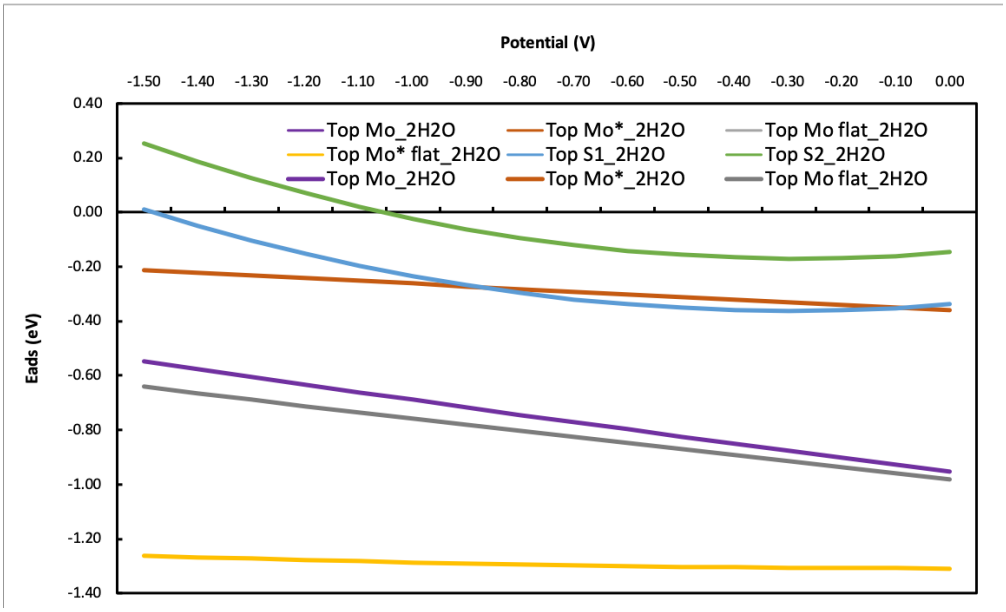

(a) Variation of the adsorption energy of the second water molecule on the different edge sites as a function of the electrochemical potential.

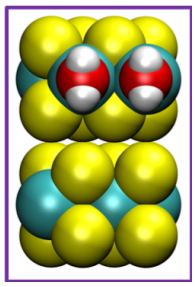

(b) Top Mo

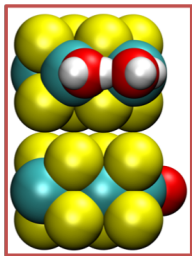

(c) Top Mo*

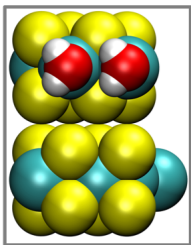

(d) Top Mo flat

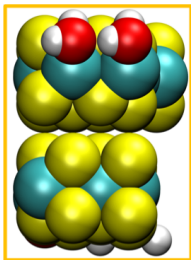

(e) Top Mo*flat

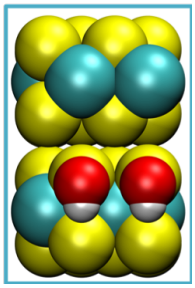

(f) Top S1

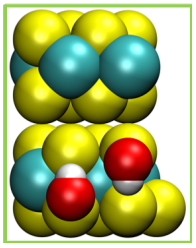

(g) Top S2

Figure S8: The adsorption energies of water on Mo and S edges with the the optimized geometry of each site. For Top S1 and Top S2, the water molecule is not very visible. In order to well visualize these two structures, see supporting information (S9).

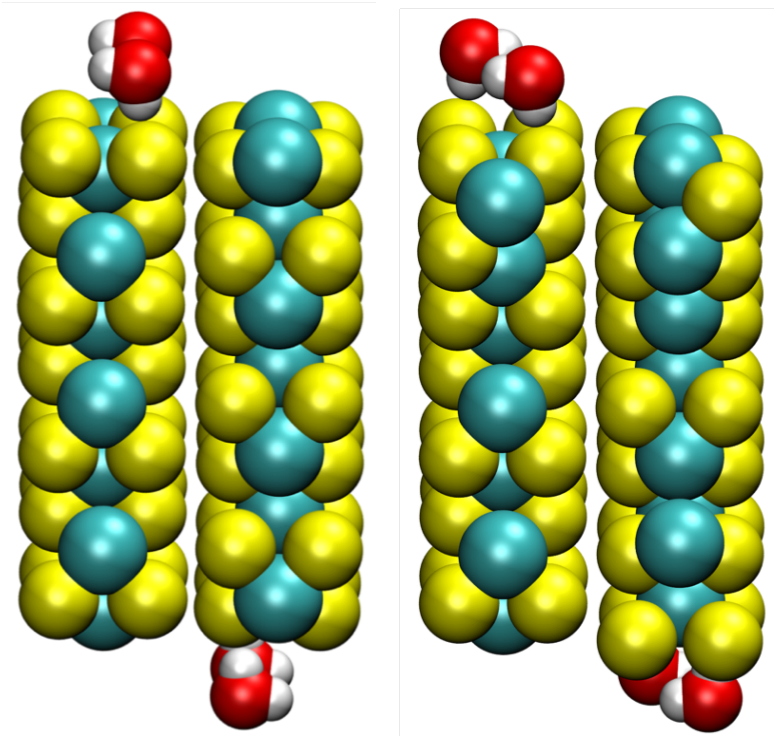

(a) Top S1 (b) Top S2

Figure S9: Adsorption of water on the Sulfur edges.

2.8 Production of H_2 from adsorbed OH and H_2O

2.8.1 OH adsorption on Mo-edges and S-edges

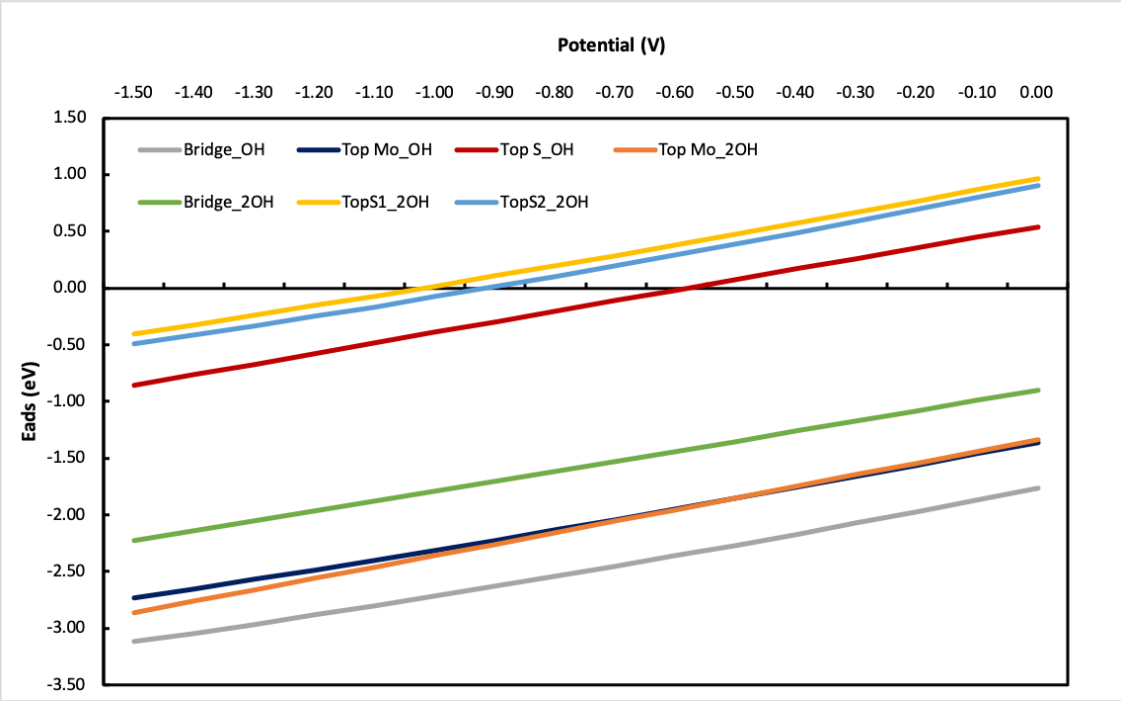

Figure S10: Variation of the adsorption energy of OH on the different edge sites as a function of the electrochemical potential

We see that for Top S, the adsorption of OH is weak with adsorption energy equal to 0.54 eV. For Top Mo and Bridge sites, the OH is strongly bound with very negative adsorption energies values further from zero (-1.36 eV and -1.77 eV respectively). With addition of the second OH on the Top Mo and Bridge sites, the adsorption energies obtained are still negative (-1.34 and -0.90 eV respectively) which means that the adsorption of second OH is also possible. For Top S1_ 2OH and Top S2_ 2OH, the addition of the second OH increases the adsorption energies values (0.97 eV and 0.91 eV respectively), so adding another OH is unlikely to occur.

To conclude, for Top Mo and Bridge sites, the adsorption of OH is very competitive with that of the hydrogen. Whereas, for the different top S sites, mostly very weak adsorption is observed mainly with adding the second OH.

2.8.2 OH/H_2O cycling without co-adsorbates: First cycle

The first possibility for HER involving adsorbed OH and water is assessed in the absence of co-adsorbates. The results for the corresponding ΔG_1, ΔG_2 and thermodynamic overpotential η_{TD} are summarized in Table S2.

Table S2: The thermodynamic overpotential η_{TD} and Gibbs free energies for each reaction step for HER at this potential for different adsorption sites in the absence of co-adsorption.

Type of site	ΔG_1 (eV)	ΔG_2 (eV)	η_{TD} (V)
Top Mo	0.02	-1.22	0.6
Top Mo flat	0.02	-1.22	0.6
Top Mo*	-0.02	-0.98	0.5
Top Mo* flat	0.01	-0.61	0.3
Top S	-1.38	-0.02	0.7
Bridge	-0.02	-2.18	1.1

An over-potential of 0.3 V must be applied in the case of Top Mo* flat. Therefore, the course of the first cycle for the production of H_2 from H_2O and OH on this site is realizable and the site is not blocked (see Figure S11(a)).

For Top Mo*, the over-potential required is a little strong (0.5 V) but remains in the range of acceptable values.

The rest of the sites are inactive because the values of the electrochemical potential to produce H_2 are high (from 0.6 V to 1.1 V). Indeed, Top Mo, Top Mo flat and Bridge are blocked by OH. For all these sites, ΔG_2 is much less than 0 eV (from -0.98 eV to -2.18 eV). For the Top S, ΔG_1 is equal to -1.38 eV which indicates the stability of H_2O and therefore the cycle stops at this stage and there is no production of H_2.

To conclude, most of the sites on the edges form strong bonds with either OH or H_2O and the first cycle which takes advantage of the presence of these two species and uses them to produce H_2 can only perform in the case of Top Mo* flat and Top Mo*.

2.8.3 OH/H_2O cycling with OH co-adsorption: Second cycle

We move to the reactivity of the second cycle on the surface of our catalyst, which involves the co-adsorption of OH. We calculate the corresponding ΔG_1 and ΔG_2 for all the tested sites except Top S1 and Top S2 where the adsorption of the second OH to start the catalytic cycle is too unfavorable and report the obtained values in Table S3).

Table S3: The thermodynamic overpotential η_{TD} and Gibbs free energies for each reaction step for HER at this potential for different adsorption sites in the presence of co-adsorbed OH.

Type of site	ΔG_1 (eV)	ΔG_2 (eV)	η_{TD} (V)
Top Mo	0.03	-1.03	0.5
Top Mo flat	-1.16	-0.04	0.6
Top Mo*	-0.38	-0.02	0.2
Top Mo* flat	-0.38	-0.02	0.2
Bridge	-0.44	0.04	0.2

We observe that for all the sites on molybdenum and for the Bridge, the over-potential to be applied is close to 0 (0.2 V) so the cycle can occur except for Top Mo and Top Mo flat. The Top Mo requires an over-potential of 0.5 V, higher than the others but remains in the accepted range which is not the case for the Top Mo flat with an over-potential equal to 0.6 V.

2.8.4 OH/H_2O cycling with co-adsorbed H_2O: Third cycle

Finally, we evaluate the third cycle, which is the HER on the edges in the presence of co-adsorbed H_2O. The corresponding results are presented in the Table S4.

We observe that this cycle requires a high over-potential in order to produce hydrogen on the edge sites except for Top Mo* flat with 0.5 V. The different steps of the cycle are presented in Figure S11 (b).

Table S4: The thermodynamic overpotential η_{TD} and Gibbs free energies for each reaction step for HER at this potential for different adsorption sites in the presence of co-adsorbed H_2O.

Type of site	ΔG_1 (eV)	ΔG_2 (eV)	η_{TD} (V)
Top Mo	0.02	-1.22	0.6
Top Mo flat	0.78	-3.78	1.5
Top Mo*	0.45	-3.45	1.5
Top Mo* flat	0.02	-1.02	0.5
Top S1	-1.03	0.03	0.9
Top S2	-1.84	0.04	1.3

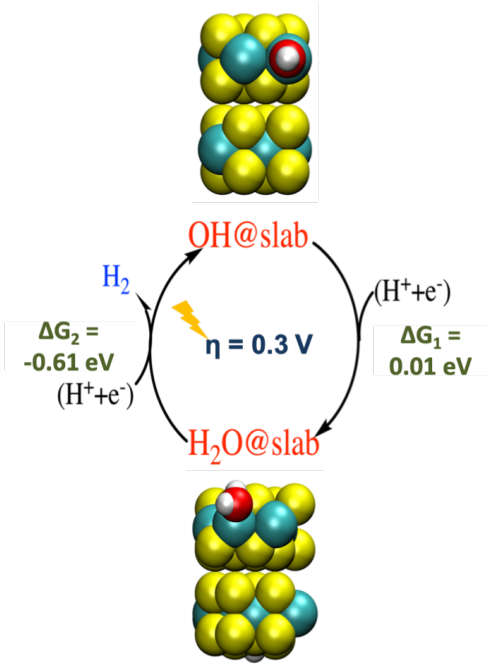

(a) The first cycle

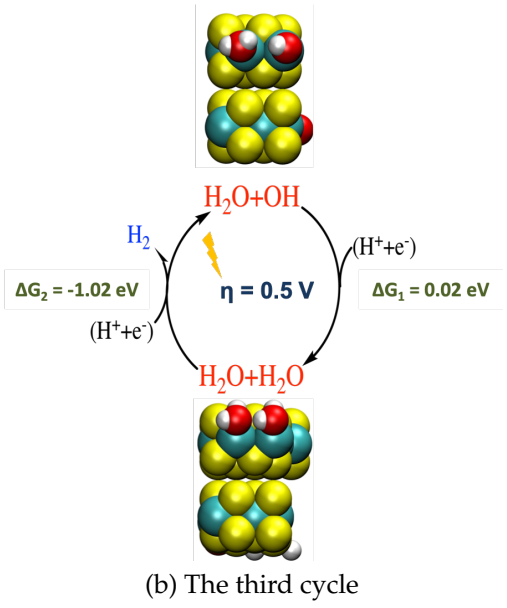

(b) The third cycle

Figure S11: The production of H_2 from H_2O and OH on the Top Mo*flat site.

References

(S1) Zhao, W.; Pan, J.; Fang, Y.; Che, X.; Wang, D.; Bu, K.; Huang, F. Metastable MoS2 : Crystal Structure, Electronic Band Structure, Synthetic Approach and Intriguing Physical Properties. *Chemistry - A European Journal* **2018**, *24*, 15942–15954.

(S2) Frondel, J. W.; Wickman, F. E. Molybdenite polytypes in theory and occurrence. II. Some naturally-occurring polytypes of molybdenite. *American Mineralogist: Journal of Earth and Planetary Materials* **1970**, *55*, 1857–1875.

(S3) Song, I.; Park, C.; Choi, H. C. Synthesis and properties of molybdenum disulphide: From bulk to atomic layers. *RSC Advances* **2015**, *5*, 7495–7514.

(S4) Heising, J.; Kanatzidis, M. G. Structure of restacked MoS2 and WS2 elucidated by electron crystallography. *Journal of the American Chemical Society* **1999**, *121*, 638–643.

(S5) Lau, T. H.; Wu, S.; Kato, R.; Wu, T. S.; Kulhavý, J.; Mo, J.; Zheng, J.; Foord, J. S.; Soo, Y. L.; Suenaga, K. et al. Engineering Monolayer 1T-MoS2 into a Bifunctional Electrocatalyst via Sonochemical Doping of Isolated Transition Metal Atoms. *ACS Catalysis* **2019**, *9*, 7527–7534.

(S6) Hu, T.; Li, R.; Dong, J. A new (2 x 1) dimerized structure of monolayer 1T-molybdenum disulfide, studied from first principles calculations. *Journal of Chemical Physics* **2013**, *139*, 174702.